

Analysis of Cells Proliferation and MicroRNAs Expression Profile in Human Chondrosarcoma SW1353 Cells Exposed to Iodine-125 Seeds Irradiation

Dose-Response:
An International Journal
April-June 2020:1-10
© The Author(s) 2020
Article reuse guidelines:
sagepub.com/journals-permissions
DOI: 10.1177/1559325820920525
journals.sagepub.com/home/dos



Fusheng Li^{1,2}, Jia Xu³, Yue Zhu¹, Liang Sun⁴, and Renyi Zhou¹

Abstract

Chondrosarcoma is the second most common bone malignancy in adults, and it is often resistant to traditional chemotherapy and radiation therapy. Permanent implantation of iodine-125 (¹²⁵I) seeds has been explored for the treatment of many types of cancer. In this study, the aim was to investigate the proliferative and microRNA (miRNA) effects of ¹²⁵I seeds irradiation on human chondrosarcoma SW1353 cells. First, a new in vitro ¹²⁵I seed irradiation model was established, and cell viability and miRNA microarray assays were performed before and after exposure to the ¹²⁵I seeds. Cell proliferation was inhibited, and miRNA expression was substantially altered by irradiation exposure. The inhibition of cell proliferation was positively correlated with increased radiation doses, with cells showing the highest total radiation dose 7 days after irradiation. A total of 2549 miRNAs were detected in the SW1353 cells after exposure to 6 Gy of radiation, which included 189 differentially expressed miRNAs (98 upregulated and 91 downregulated). Four miRNAs were found to play important roles in the inhibition of cell proliferation after irradiation exposure, including miR-1224-5p, miR-492, miR-135b-5p, and miR-6839-5p. The target genes of the associated miRNAs mentioned were vascular endothelial growth factor A (VEGFA), C-X-C motif chemokine 12 (CXCL12), mitogen-activated protein kinase kinase kinase 3 (MAP4K3), and apoptosis facilitator Bcl-2-like protein 14 (BCL2L14). Hence, the mitogen-activated protein kinase signaling pathway may be involved in how chondrosarcoma cells respond to ¹²⁵I seed irradiation.

Keywords

chondrosarcoma, iodine-125, irradiation, microRNAs, proliferation

Introduction

Chondrosarcoma is a heterogeneous group of malignancies, characterized by the production of a significant amount of extracellular matrix by tumor cells.¹ Currently, chondrosarcoma is the second most common bone malignancy in adults. Surgical resection is the preferred treatment for patients with chondrosarcoma, as the tumors are often resistant to conventional chemotherapy and radiotherapy. However, radiotherapy may still be used for treating positive surgical margins or inoperable tumors in difficult anatomical sites, such as the base of the skull or sacrum.^{1,2}

Permanent implantation of iodine-125 (¹²⁵I) seeds is a kind of brachytherapy. The radioactive ¹²⁵I seeds emit γ -rays at 29 keV, which effectively destroy the double strands of DNA in tumor nuclei, resulting in the loss of proliferative abilities. The average radiation radius of ¹²⁵I seeds is 1.7 cm, which limits the off target damage to surrounding tissues when the seeds are

¹ Department of Orthopaedics, The First Affiliated Hospital of China Medical University, Shenyang, People's Republic of China

² Department of Orthopaedic Oncology, The People's Hospital of Liaoning Province, China Medical University People's Hospital, Shenyang, People's Republic of China

³ Clinical Teaching Experimental Center, Key Laboratory of Environmental Pollution and Microecology of Liaoning Province, Shenyang Medical College, Shenyang, People's Republic of China

⁴ State Key Laboratory of Radiation Medicine and Protection, School of Radiation Medicine and Protection, Soochow University, Suzhou, People's Republic of China

Received 05 November 2019; accepted 11 March 2020

Corresponding Author:

Yue Zhu, Department of Orthopaedics, The First Affiliated Hospital of China Medical University, 155 Nan Jing Bei Street, Shenyang 110001, People's Republic of China.

Email: zhuyuedr@163.com



Creative Commons Non Commercial CC BY-NC: This article is distributed under the terms of the Creative Commons Attribution-NonCommercial 4.0 License (<https://creativecommons.org/licenses/by-nc/4.0/>) which permits non-commercial use, reproduction and distribution of the work without further permission provided the original work is attributed as specified on the SAGE and Open Access pages (<https://us.sagepub.com/en-us/nam/open-access-at-sage>).

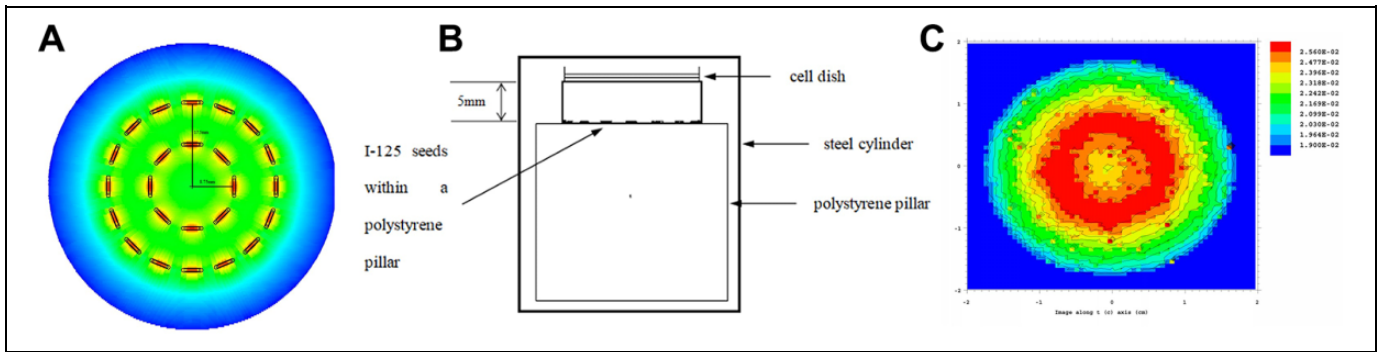


Figure 1. Development of an in vitro iodine-125 (^{125}I) seed irradiation model. A, Arrangement of 24 ^{125}I seeds onto the surface of a polystyrene pillar. Sixteen seeds were equally placed around the circumference of a 17.5-mm radius, and 8 seeds around the circumference of an 8.75-mm radius. B, The ^{125}I seed irradiation model of cells. C, Differences in the irradiation dose distribution at various points on the treatment cell plane were less than 10%.

implanted into the tumor.^{3,4} It was previously shown that cells in different phases of the cell cycle display differences in radiation sensitivity, with cells in the G2/M phase being most sensitive to irradiation. The long half-life of ^{125}I seeds ($t_{1/2} = 59.4$ days) allows for the continuous release of γ -rays at the site of placement. Nowadays, interstitial implantation of ^{125}I seeds has been used to treat prostate cancer, and some other forms of recurrent or inoperable malignancies, such as non-small cell lung cancer, pancreatic cancer, and intracranial gliomas.⁴⁻⁸ Previously, Ren et al³ reported the use of ^{125}I seeds placed into the resected tumor bed of a patient with recurrent lumbar vertebral chondrosarcoma who underwent marginal resection. Although the pathology specimen was showed conventional low-grade chondrosarcoma, the treatment was effective, with no signs of recurrence at the 2-year follow-up. Hence, ^{125}I seed implantation may be an effective approach for the treatment of inoperable chondrosarcomas.

MicroRNAs (miRNAs) are a class of endogenous, small noncoding RNAs that serve as regulators of gene expression in multicellular organisms. MicroRNAs can affect the output of many protein-coding genes and negatively regulate the translation of messenger RNAs (mRNAs) by attaching to complementary base pairs of the target genes, leading to effective degradation of mRNAs.⁹⁻¹² Some studies have demonstrated that miRNAs play an important role in the proliferation, invasion, and metastasis of cancer.¹³⁻²²

In recent years, several studies have assessed the roles of miRNAs in chondrosarcoma, yet none of the findings have focused on the effects of ^{125}I seeds irradiation exposure on the miRNAs expression profiles of conventional chondrosarcoma cells.^{12,23-27} In the current study, we developed a new in vitro ^{125}I seed irradiation model to study the effects of ^{125}I seed irradiation on the proliferation of grade II chondrosarcoma SW1353 cells. Microarray analysis was performed to detect the miRNAs expression profiles of irradiated and nonirradiated cells. We hypothesized that miRNAs, which are significantly altered after exposure to irradiation from ^{125}I seeds, may play an important role in the cell response network. In addition, we conducted an integrative analysis of miRNAs–mRNAs

regulatory networks, which could improve our understanding of ^{125}I seed brachytherapy in the treatment of chondrosarcoma.

Materials and Methods

Establishment of an In Vitro ^{125}I Seed Irradiation Model

Iodine-125 seeds were provided by Beijing Zhibo Bio-Medical Technology Co, Ltd (Beijing, China). The ^{125}I seeds were placed onto the surface of a polystyrene pillar, which was 50 mm high and 50 mm diameter. Next, 16 seeds were placed equally around the circumference of a 17.5-mm radius, and 8 seeds around the circumference of an 8.75-mm radius (Figure 1A). The cell dish was 5 mm away from the top of the pillar, which contained 24 seeds (Figure 1B). When in use, the irradiator was placed in a cylindrical container manufactured with 3-mm-thickness steel, which had 4 ventilation holes in the upper sidewall (diameter = 5 mm). The initial activity of the ^{125}I seed was 0.8 mCi. The Monte-Carlo model was used to calculate the dose distribution at various points on the cell plane. The initial mean dose was also calculated. The differences in irradiation dose distribution at various points on the cell plane were less than 10% (Figure 1C). As calculated, the initial mean dose rate (D_0) was 7.802 cGy/h. The total dose (D_t) in a certain length of irradiation exposure could be calculated using the following calculation.

$$D_t = D_0 \int_{t=0}^{t=T} e^{-\lambda t} dt$$

In the equation, t is time in hours, λ is the decay constant for ^{125}I , and T is the length of irradiation (hours). For the calculation, $t_{1/2} = 1425.6$ hours (59.4 days). Alternatively, the length of irradiation exposure could also be calculated if the total dose was given.²⁸

Cell Culture

The human chondrosarcoma SW1353 cell line was purchased from ZiShi Biotech Co, Ltd (Shanghai, China). The cells were

Table 1. List of Primers for qRT-PCR.

MiRNAs	Forward	Reverse
U6	GTAACCACCTTGGTGTCTTGTCC	GGCCAACCGCGAGAAGATGTTTTTTTTT
hsa-miR-492	AGGACCTGCGGGACAAGATTCTT	GGCCAACCGCGAGAAGATGTTTTTTTTT
hsa-miR-135b-5p	CCGGGTATGGCTTTTCATTCTATGTGA	GGCCAACCGCGAGAAGATGTTTTTTTTT
hsa-miR-1224-5p	GTGAGGACTCGGGAGGTGG	GGCCAACCGCGAGAAGATGTTTTTTTTT
hsa-miR-1469	ATTTCTCGGCGCGGGGCGCGG	GGCCAACCGCGAGAAGATGTTTTTTTTT
hsa-miR-22-5p	CGGAGTTCTTCAGTGGCAAGCTTTA	GGCCAACCGCGAGAAGATGTTTTTTTTT
hsa-miR-5196-3p	TCATCCTCGTCTCCCTCCCA	GGCCAACCGCGAGAAGATGTTTTTTTTT
hsa-miR-4689	TTGAGGAGACATGGTGGGGG	GGCCAACCGCGAGAAGATGTTTTTTTTT
hsa-miR-4746-3p	ATTTAGCGGTGCTCCTGCGGG	GGCCAACCGCGAGAAGATGTTTTTTTTT
hsa-miR-6076	AGCATGACAGAGGAGAGGTGG	GGCCAACCGCGAGAAGATGTTTTTTTTT
hsa-miR-6839-5p	AGTCTGGATTGAAGACGACCCCA	GGCCAACCGCGAGAAGATGTTTTTTTTT
GAPDH	GGAGCGAGATCCCTCCAAAAT	GGCTGTTGTCATACCTTCATGG
VEGFA	GCCTTGCCCTTGCTGCTCTACC	GGTCTCGATTGGATGGCAGTAGC
MAPK1	ACCAGACCTACTGCCAGAGAACC	TGGTCATTGCTGAGGTGTTGTGTC
CUL3	GACAAATCAACGGAAGAACCAA	TCCTTCTTCAGAAACAAGAGCT
HNRNP1	AATACCATACTGTGAATGGCCA	CCAAAGTTTCCAGAACCCTTC
PPP1CC	TCCAGCTTCAGGAGAATGAAAT	TGGTGCTTCAAGTTCTAGTAGG
CXCL12	TCGTGGTCTGCTGGTCTCTC	TTGAGATGCTTGACGTTGGCTCTG
BCL2L14	GTGGAGAAGGAAGATTCCGAGAGC	TTGAGATGCTTGACGTTGGCTCTG
MAP4K3	TGATGATCCTGAGCCTTGTGTGC	GTAACCACCTTGGTGCATCTGTCC
FGFR1	GTGGTGTGGCAGAGCTATCG	TGCGTCCGACTTCAACATCTTCAC
BCL2L1	CGGGCATTCACTGACCTGAC	ACTGAAGAGTGAGCCCAGCA

Abbreviations: miRNAs, microRNAs; qRT-PCR, quantitative real-time polymerase chain reaction.

cultured in Dulbecco modified Eagle medium supplemented with 10% fetal bovine serum (Pan Biotech, Aidenbach, Germany), 100 U/mL penicillin, and 0.1 mg/mL streptomycin. A humidified incubator with 5% CO₂ was maintained at 37°C. For the extraction of RNA, the cells were seeded into 3.5 cm culture plates and grown to 85% confluency.

Iodine-125 Seed Irradiation

Human chondrosarcoma SW1353 cells were divided into experimental (irradiated) and control (nonirradiated) groups. The experimental groups were set up with a total dose of 2, 4, 6, and 8 Gy. In the current study, there were 3 samples in the irradiated and control groups, respectively.

Cell Viability Assay

Cells were seeded in 96-well plates at 1200 or 2500 cells/well according to the postirradiated cultured time. The adherent cells were cultured for 24 hours and then irradiated by the ¹²⁵I seeds. After irradiation, 3 wells were detected in each group per day for a period of 7 days. The absorbance at 570 nm (optimal density or OD) was measured using the SpectroMax190 (Molecular Devices, San Jose, California) according to the manufacturer's instructions. The curve depicting the cell growth inhibition was established, and the cell growth inhibition rate was calculated using this formula: 1 – (irradiated group OD/control group OD) × 100%. Experiments were performed in triplicate for statistical analysis.

RNA Isolation and Microarray Analysis

After the cells were treated with a total dose of 6-Gy irradiation, the RNA was extracted from SW1353 cells in the experimental and control groups within 1 hour after irradiation. The samples were obtained and purified using the MagMAX mirVana Total RNA Isolation Kit (Thermo Fisher Scientific, Waltham, Massachusetts). Subsequently, the NanoDrop 2000 Spectrophotometer (Thermo Fisher Scientific) was applied to measure the quality and quantity of total RNA at the absorbance of 260 nm. Finally, the miRNAs expression profiles were detected using the Agilent Human miRNA Microarray (Oebiotech, Shanghai, China), which contained 2569 miRNA probes.

Bioinformatics Analysis

Agilent's Feature Extraction version 10.7.1.1 software (Santa Clara, California) was used to extract the original data obtained after chip hybridization. Next, the original data were standardized using the quantile method. The GeneSpring GX version 13.1 software (Agilent) was used for target gene prediction. TargetScan (<http://www.targetscan.org/>), PITA (http://genie.weizmann.ac.il/pubs/mir07/mir07_data.html), and microRNA.org online databases were used to predict the target genes of differential miRNAs. The target genes were selected for subsequent Gene Ontology (GO; <http://www.geneontology.org>) and Kyoto Encyclopedia of Genes and Genomes (KEGG; <http://www.genome.jp/kegg/>) analysis to determine their primary functions. The GO included 3 major modules, including biological processes, cellular components, and molecular functions, leading to 3 results. The pathway analysis of

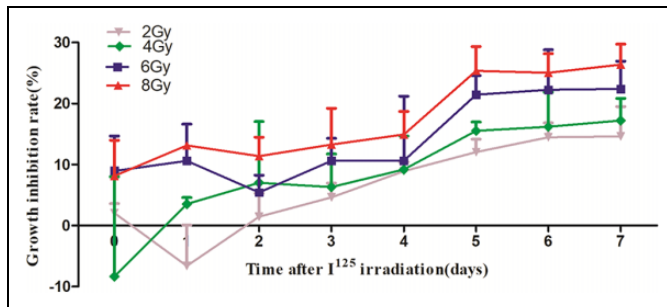


Figure 2. Inhibition of SW1353 cell growth after exposure to iodine-125 irradiation. The inhibition of cell growth was dose dependent and reached the highest levels at 7 days postirradiation. The rates for the 2, 4, 6, and 8 Gy groups were 14.64%, 17.25%, 22.41%, and 26.39% at 7 days postexposure, respectively ($P < .05$).

the target genes was conducted in the KEGG database, which played a crucial role in isolating the target genes enriched in each pathway. Value of $P < .05$ was used as the cutoff value for both GO and KEGG pathway analyses.

The protein-protein interactions (PPIs) network of predicted target genes was constructed by STRING (<http://www.string-db.org>) and visualized by Cytoscape software version 3.7.1 (<https://www.cytoscape.org>). The MCODE plug-in for Cytoscape was used to analyze the whole PPI network with a degree cutoff of 2, haircut cluster finding, node score cutoff of 0.2, k-core of 2, and a maximum depth of 100.²⁹ The cutoff criteria to search for the key molecules in the SW1353 cells treated with ¹²⁵I seeds were greater than 15.

Quantitative Real-Time Polymerase Chain Reaction Analysis

Quantitative real-time polymerase chain reaction (qRT-PCR) was conducted to validate the results of the miRNAs microarray analysis, along with the predicted target genes. Equal amounts of total RNA from each sample used in the miRNA microarray assay were reverse transcribed using the miRNA First-Strand cDNA Synthesis (Tailing Reaction; Sangon Biotechnology Co Ltd, China) and PrimeScript RT Reagent Kit with gDNA Eraser (Perfect Real Time) from Takara Bio Inc, (Shiga, Japan). The qRT-PCR was monitored using the ABI PRISM 7500 Sequence Detection System (Applied Biosystems, Foster City, California). The experiment was run in triplicate. All levels were normalized to GAPDH, and fold induction was calculated by setting the control conditions to 1. The primers are given in Table 1.

Statistical Analysis

Statistical analysis of the miRNA microarray data involved the 1-way analysis of variance using the Affymetrix Expression Console TAC (Santa Clara, California), followed by the least significant difference test. Statistics for qRT-PCR were performed with the Student *t* test using SPSS version 16.0 software

(IBM, Chicago, Illinois), and significant differences were considered at $P < .05$.

Results

Iodine-125 Seed Irradiation Inhibits the Proliferation of Chondrosarcoma Cells

The growth inhibition rates of cells exposed to 2, 4, 6, and 8 Gy of radiation were calculated to investigate the effects of ¹²⁵I seed irradiation on the proliferation of chondrosarcoma cells. In SW1353 cells, cell growth became unstable for 2 days after exposure to 2 Gy irradiation, followed by a gradual increase in the percentage of cell growth inhibition to 7 days postexposure. In the group exposed to 4 Gy of radiation, a gradual increase in cell growth inhibition was seen from after the first day to 7 days postexposure. However, the inhibition rates experienced in the 6 and 8 Gy groups were nearly instantaneous, with cell growth being inhibited the first day after irradiation. As the radiation dose increased from 2 to 8 Gy, the percentage of cell growth inhibition also increased, reaching the highest value by 7 days postexposure. As shown in Figure 2, the rates of cell growth inhibition for the 2, 4, 6, and 8 Gy groups were 14.64%, 17.25%, 22.41%, and 26.39% at 7 days postirradiation, respectively ($P < .05$).

Differential Expression of MiRNAs in SW1353 Cells After Irradiation

In the SW1353 cells exposed to 6 Gy of radiation, the microarray analysis identified 2549 total miRNAs. As compared with the control group, there were 189 differentially expressed miRNAs ($P < .05$), including 98 upregulated and 91 downregulated miRNAs (Figure 3A). The top 15 differentially expressed upregulated and downregulated miRNAs between the irradiated and control groups are listed in Tables 2 and 3, respectively. The clustering histogram revealed the different miRNAs expression profiles between the irradiated group and control group, and the heatmap showed the top 15 differentially expressed miRNAs between irradiated and nonirradiated groups (Figure 3B).

Predicted Target Genes and MiRNA-Gene Networks Analysis

As the primary function of miRNAs is to repress the expression of target genes,³⁰ the correlated miRNA-target pairs were simultaneously predicted using the TargetScan, PITA, and miRNA.org databases (Figure 4A). We selected the intersection of the 3 databases to predict the target genes, and there are only 3 miRNAs (miR-1224-5p, miR-492, and miR-135b-5p) which have target genes in the intersection. Based on the target gene predictions, the miRNA-mRNA regulatory interaction network was visualized between the 3 miRNAs and 375 mRNAs (Figure 4B).

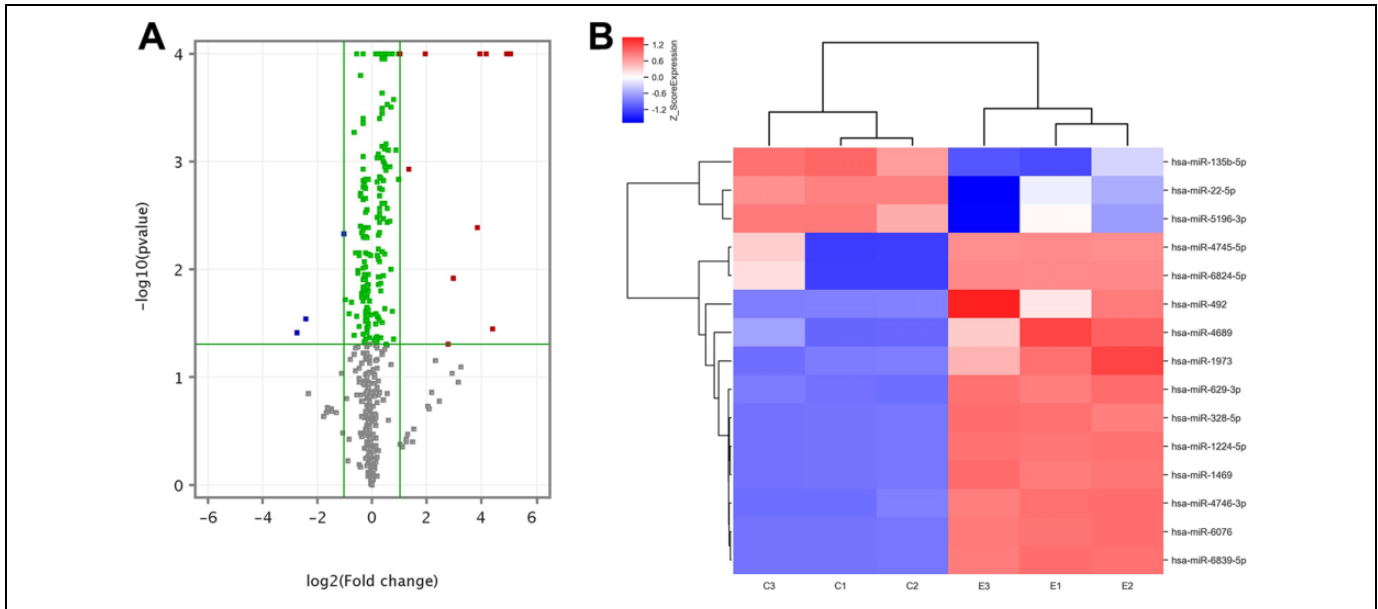


Figure 3. Differentially expressed microRNAs (miRNAs) in SW1353 cells exposed to iodine-125 (^{125}I) seeds. A, Volcano plot. Vertical green lines: 2-fold changes of difference multiple between the experimental and control group; horizontal green line: $P = .05$. Gray dots represent the miRNAs with $P > .05$. Green dots represent miRNAs with fold-change < 2 and $P < .05$. Red dots represent the miRNAs with fold-change > 2 and $P < .05$, which are significantly upregulated differential miRNAs. Blue dots represent the miRNAs with fold-change < -2 and $P < .05$, which are significantly downregulated differential miRNAs. B, Hierarchical cluster analysis of the top 15 differentially expressed upregulated and downregulated miRNAs in SW1353 cells exposed to ^{125}I seeds. Red indicates high relative expression, while blue indicates low relative expression.

Table 2. Top 15 Differentially Expressed Upregulated MiRNAs Between SW1353 Cells Exposed to Irradiation and the Control Group.

MicroRNAs	Average Expression in Control Group	Average Expression in ^{125}I Group	Fold-Change	ANOVA (P Value)
hsa-miR-6076	-3.3	1.76	33.37	.00000102
hsa-miR-6839-5p	-3.3	1.70	32.01	.00000203
hsa-miR-1224-5p	-3.3	1.63	30.54	.000000051
hsa-miR-6824-5p	-1.87	2.55	21.44	.03580002
hsa-miR-1469	-3.3	0.89	18.27	.000000798
hsa-miR-328-5p	-3.3	0.63	15.30	.000000478
hsa-miR-4689	-3.01	0.84	14.39	.004125495
hsa-miR-492	-3.3	-0.33	7.84	.012121474
hsa-miR-4745-5p	-2.29	0.49	6.89	.049530223
hsa-miR-629-3p	0.44	2.41	3.91	.00000143
hsa-miR-1973	1.61	2.96	2.56	.001193884
hsa-miR-4746-3p	3.09	4.13	2.06	.00000341
hsa-miR-4485-3p	3.28	4.25	1.96	.0000299
hsa-miR-135a-3p	1.52	2.48	1.95	.001470052
hsa-miR-4428	2.28	3.14	1.81	.000804

Abbreviations: ANOVA, 1-way analysis of variance; ^{125}I , iodine-125; miRNA, microRNA.

Gene Ontology Analysis of Predicted Target Genes

The relationship between predicted target genes and their functions was successfully uncovered through the GO analysis. The calculation returned an enriched P value, and a smaller P value indicated a higher degree of enrichment of the target gene in the GO term. In the GO analysis, there were 145 different biological processes, 36 different cellular components, and 46 different molecular functions identified, based on $P < .05$. The top 20 biological processes, cellular

component, and molecular function GOs are shown in Figure 5A to C, respectively.

Pathway Analysis of Predicted Target Genes

The top 20 significant pathways of predicted target genes were identified based on the KEGG database, including proteoglycans in cancer, the mitogen-activated protein kinase (MAPK) signaling pathway, cysteine and methionine metabolism, long-

Table 3. Top 15 Differentially Expressed Downregulated MiRNAs Between SW1353 Cells Exposed to Irradiation and the Control Group.

MicroRNAs	Average Expression in Control Group	Average Expression in ¹²⁵ I Group	Fold-Change	ANOVA (P Value)
hsa-miR-5196-3p	1.02	-1.69	-6.58	.038893394
hsa-miR-22-5p	0.47	-1.92	-5.23	.02877958
hsa-miR-135b-5p	1.70	0.69	-2.01	.004806157
hsa-miR-18a-5p	0.94	-0.03	-1.96	.01941451
hsa-miR-21-3p	2.81	1.98	-1.78	.026309982
hsa-miR-4640-3p	1.47	0.71	-1.68	.020299722
hsa-miR-6732-3p	1.38	0.72	-1.58	.041156914
hsa-miR-4284	7.77	7.11	-1.58	.00055
hsa-miR-29b-1-5p	2.86	2.26	-1.52	.007111116
hsa-miR-523-3p	1.63	1.08	-1.46	.027703047
hsa-miR-424-5p	5.11	4.57	-1.45	.0000208
hsa-miR-19a-3p	3.44	2.91	-1.44	.010547455
hsa-miR-503-5p	2.01	1.50	-1.43	.010960225
hsa-miR-210-3p	3.75	3.27	-1.39	.03419331
hsa-miR-512-5p	3.78	3.31	-1.39	.007449524

Abbreviations: ANOVA, 1-way analysis of variance; ¹²⁵I, iodine-125; miRNAs, microRNAs.

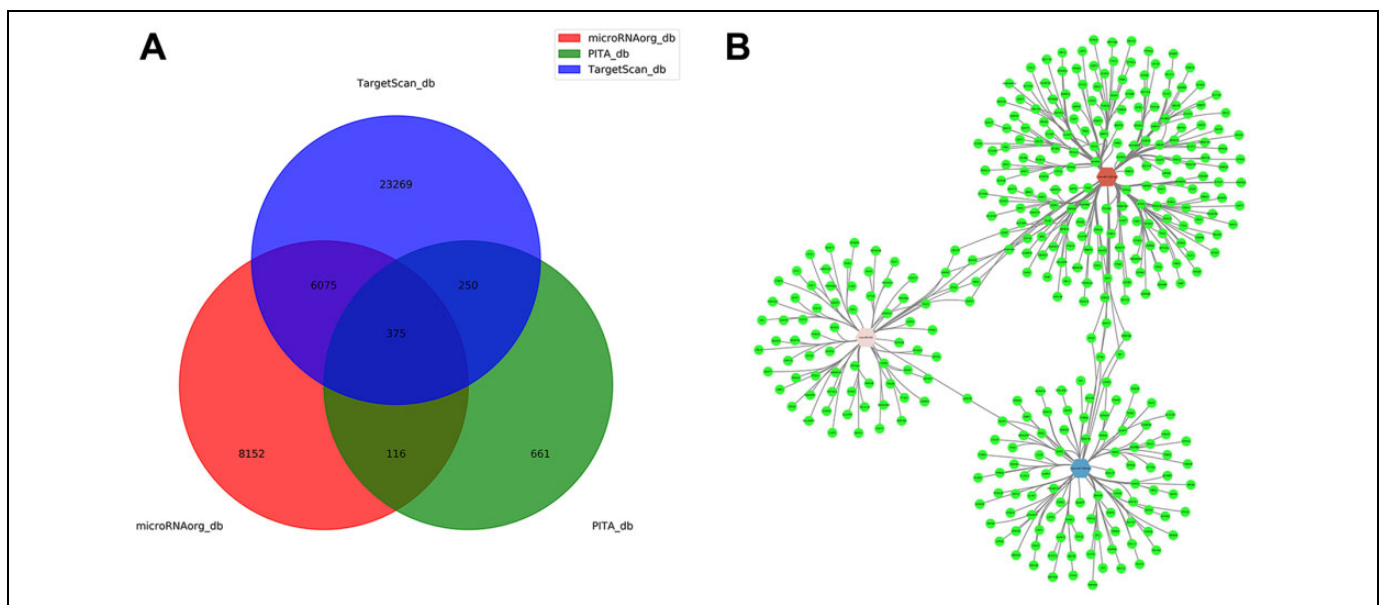


Figure 4. Network of microRNA (miRNA) and predicted target gene. A, Target genes database prediction of differential miRNAs. B, MicroRNA target gene network. Green nodes stand for target genes. Hexagon nodes represent miRNAs (red node indicate upregulated, the fold-change = 30.54; pink node indicate upregulated, the fold-change = 7.84; blue node indicate downregulated, the fold-change = -2.01). The lines represent the regulatory relationship between the miRNAs and target genes.

term potentiation, axon guidance, prion diseases, the insulin signaling pathway, the ErbB signaling pathway, breast cancer, adrenergic signaling in cardiomyocytes, central carbon metabolism in cancer, the cyclic adenosine monophosphate (cAMP) signaling pathway, epidermal growth factor receptor tyrosine kinase inhibitor resistance, pathways in cancer, the transforming growth factor β signaling pathway, acute myeloid leukemia, regulation of actin cytoskeleton, the gonadotropin-releasing hormone signaling pathway, oocyte meiosis, and the P13k-Akt signaling pathway (Figure 5D). The genes involved in these significant pathways are shown in Table 3.

Protein-Protein Interaction Networks Analysis of Predicted Target Genes

The PPI network of predicted target genes was constructed by STRING and visualized by Cytoscape (Figure 6). A total of 299 genes were found to be essential genes through the screening. Moreover, the whole PPI network was analyzed by MCODE. The cutoff criterion was set to greater than or equal to 15, indicating that these genes have more interactions than less studied genes in the network. The key genes include vascular endothelial growth factor A (*VEGFA*), *MAPK1*, *CUL3*, *HNRNPA1*, and *PPP1CC*.

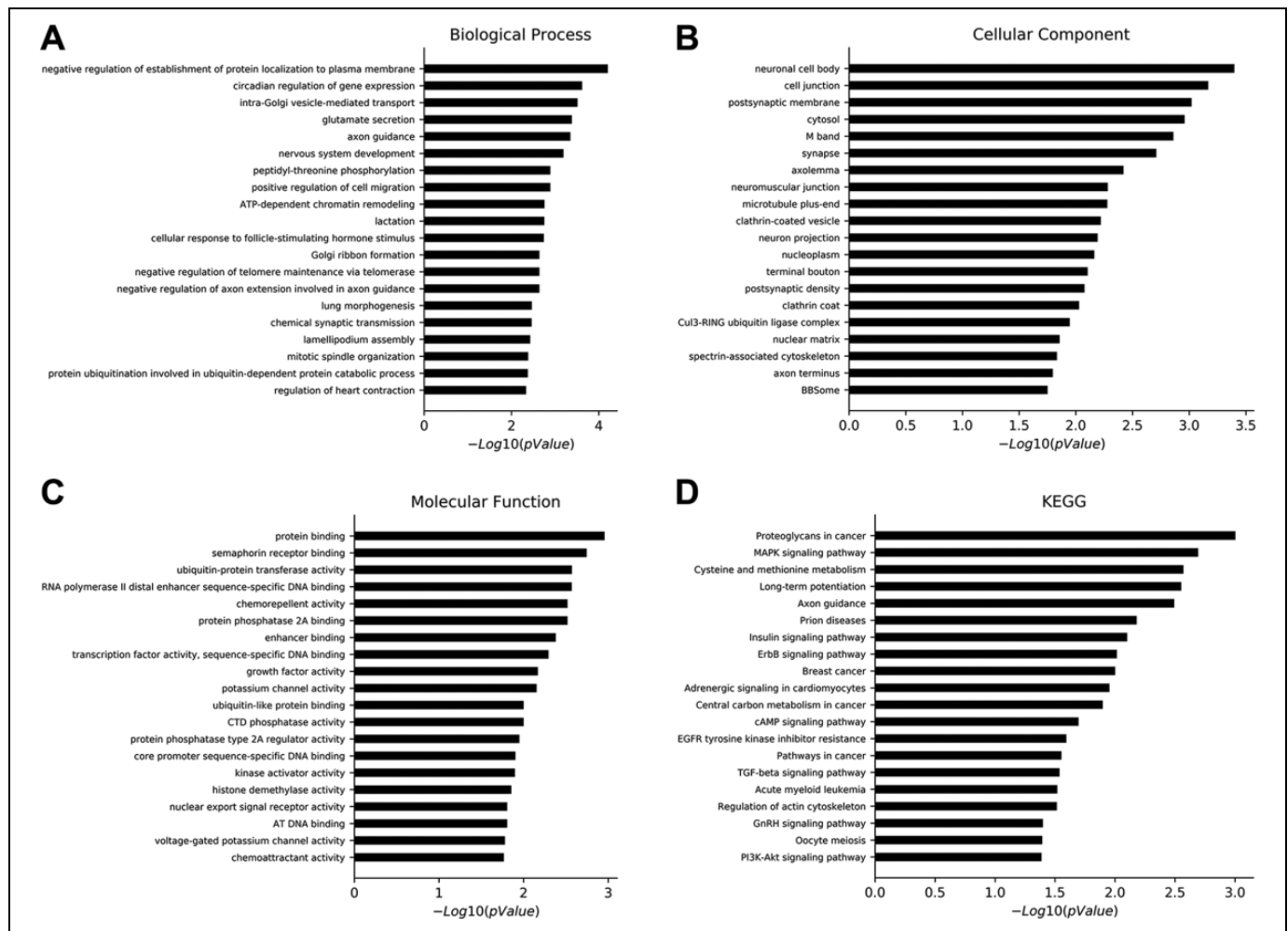


Figure 5. Gene Ontology and pathways analysis of predicted genes. A, Top 20 differential biological processes of predicted target genes in SW1353 cells exposed to iodine-125 (^{125}I) seeds. B, Top 20 differential cellular components of predicted target genes in SW1353 cells exposed to ^{125}I seeds. C, Top 20 differential molecular functions of predicted target genes in SW1353 cells exposed to ^{125}I seeds. D, Important pathways of the predicted target genes based on the Kyoto Encyclopedia of Genes and Genomes database.

Quantitative Real-Time Polymerase Chain Reaction Analysis of Differentially Expressed miRNAs and Their Target Genes

As predictions based on miRNA sequence complementarity and their target genes may cause false-positive results,³⁰ qRT-PCR was performed with 10 miRNAs and 10 predicted target genes based on the microarray, pathway, and PPI network analyses (Figure 7A and B). From the analysis, 70% (7/10) of the validated genes showed expression trends consistent with those of the microarray analysis. However, the expression levels of miR-4689, miR-6076, and miR1469 were inconsistent with the microarray analysis, yet the differences were not evident (Figure 7A).

Discussion

Grade II chondrosarcoma show high resistance to chemotherapy and radiation therapy, a metastatic potential and high

recurrence rate, all of which are suitable characteristics when thinking about developing adjuvant therapies.³¹ SW1353, JJ012, and CH3573 are currently the most characterized conventional grade II chondrosarcoma cell lines.³² Among them, SW1353 is the most extensively used and is considered as the gold standard among other cells.³³

The ^{125}I seeds primarily emit γ -rays with strong penetrating powers, leading to cell damage through the production of intermediate ions and free radicals that cause double-stranded breaks in the DNA. In our study, ^{125}I seeds inhibited the proliferation of SW1353 cells in vitro in a dose-dependent manner, with higher doses of radiation increasing the inhibition of cell growth.

Due to the integral roles of miRNAs as gene expression regulators, we hypothesized that miRNAs, which are significantly altered after exposure to irradiation from ^{125}I seeds, may play an important role in the cell response network. Among the 10 miRNAs selected for validation in our study, 4 key miRNAs, including miR-1224-5p, miR-492, miR-135b-5p, and

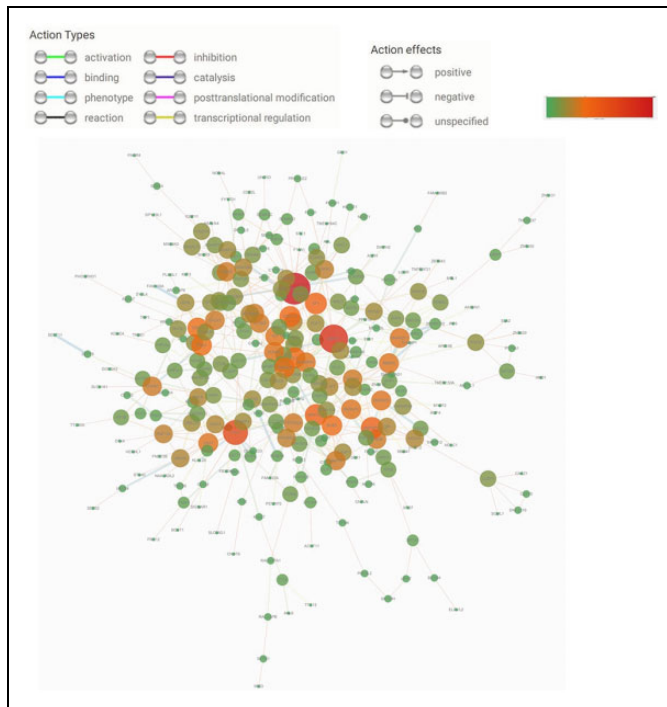


Figure 6. Protein–protein interaction networks of the target genes. The area and color of the circle represent the degree. Red represents the maximum value, and green represents the minimum value. For the interpretation of colors, please refer to the web version of this article.

miR-6839-5p, were found to be differentially expressed in the irradiated cells as compared with the control group. No previous studies have reported on the regulatory roles of miR-1224-5p, miR-492, or miR-135b-5p in chondrosarcoma cells,^{23,25-26} yet some published documents have shown that miR-1224-5p, miR-492, and miR-135b-5p may play important roles in the proliferation, invasion, and metastasis of nonchondrosarcoma tumors.¹³⁻²² To the best of our best knowledge, miR-6839-5p has not been reported in the literature. In the current study, we hypothesized that miR-1224-5p, miR-492, miR-135b-5p, and miR-6839-5p might play vital roles in how SW1353 cells respond to irradiation with ¹²⁵I seeds.

First, miR-1224-5p serves as a potential tumor suppressor in some malignancies. The upregulation of miR-1224-5p may decrease cell proliferation, induce apoptosis, inhibit migration and invasion, and suppress tube formation in the endothelial cells of human hepatocellular carcinoma (HCC).¹³ In malignant gliomas, miR-1224-5p has been shown to inhibit tumor-associated activity by targeting the cAMP response element-binding protein (*CREB1*) gene.¹⁴

Second, miR-492 promotes the progression of prostate cancer, liver cancer, hepatoblastoma, and cervical squamous cell carcinoma.¹⁵⁻¹⁸ miR-492 represses *SOCS2* expression to exert tumor-promoting functions in prostate cancer cells, which is implicated in the regulation of HCC progression through *PTEN* and *AKT* pathways. Hence, patients with HCC with high miR-492 and low *PTEN* had poorer prognoses in the clinic.¹⁵⁻¹⁶ MicroRNA-492 also regulates the metastatic potential of

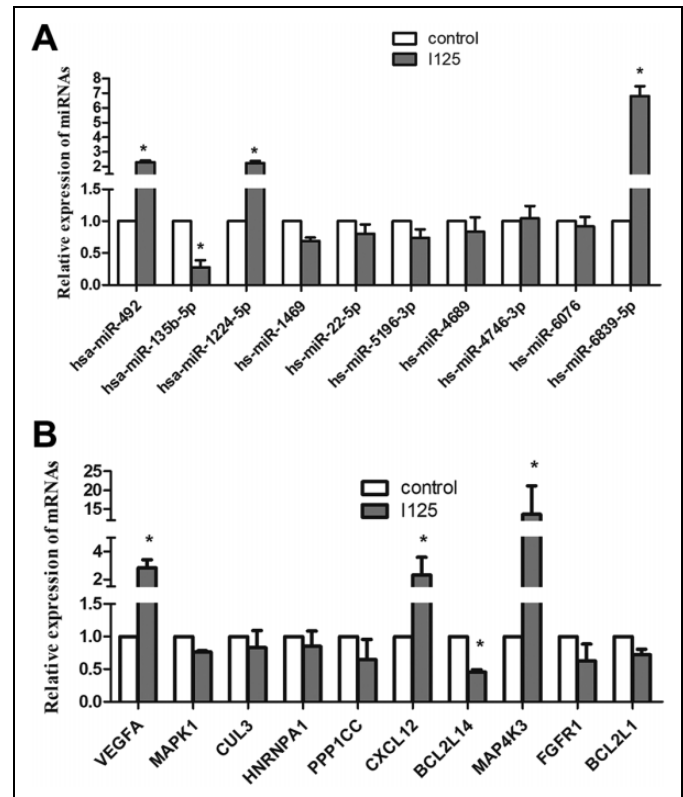


Figure 7. Quantitative real-time polymerase chain reaction analysis of 10 differential microRNAs (miRNAs) and their predicted target genes between the irradiated and control groups. A, Findings from the 10 miRNAs identified 4 key miRNAs. B, Findings from 10 predicted target genes identified 4 essential genes. * Fold-change >2 or fold-change <0.5.

hepatoblastoma via CD44 signaling.¹⁷ In cervical squamous cell carcinomas, miR-492 overexpression has been correlated with pelvic lymph nodes metastasis and was found to enhance the radiosensitivity of cells.¹⁸

Lastly, miR-135b-5p has been reported to promote carcinogenesis and tumor development in humans,¹⁹ including pancreatic ductal adenocarcinoma (PDAC) and gastric cancer.²⁰⁻²¹ The overexpression of miR-135b-5p was associated with unfavorable clinical outcomes and poor prognosis, such as regional lymph node metastases, vascular invasion, and tumor microthrombus in PDAC.²⁰ Moreover, miR-135b-5p was found to directly target frizzled-related protein 4 to regulate the Wnt/ β -catenin signaling pathway in PDAC.²⁰ Functionally, high levels of miR-135b-5p suppress apoptosis and induce cisplatin resistance in gastric cancer.²¹ On the other hand, miR-135b-5p upregulation can increase the doxorubicin sensitivity of breast cancer cells via anterior gradient 2 (*AGR2*). The overexpression of *AGR2* is involved in pathogenesis of breast cancer, including the growth and metastasis of tumors, which is associated with poor prognoses.²²

Based on the target genes prediction, PPI networks analysis, and qRT-PCR validation, *VEGFA*, C-X-C motif chemokine 12 (*CXCL12*), and *MAP4K3* were found to be upregulated in the

irradiated group, while Bcl-2-like protein 14 (*BCL2L14*) was downregulated ($P < .05$). The 4 mRNAs are the target genes of miR-1224-5p, miR-492, miR-135b-5p, and miR-6839-5p. However, one miRNA can inhibit many mRNAs, and one mRNA can also interact with many genes through different pathways. Inside tumor cells, miRNAs can act as either tumor promoters or suppressors, with additional functional alterations concerning the role of their mRNA targets.¹¹ However, we are unable to obtain the specific miRNA–mRNA pairing information from this study.

Using the KEGG database, the top 20 pathways of the target genes were identified, some of which are involved in cancer and radiation injury. In a previous study, Dent et al³⁴ showed that several proteins in the MAPK pathway have critical roles in how cells respond to radiation exposure. Since *MAPK1* and *MAP4K3* were predicted target genes of the miRNAs differentially expressed in the irradiated cells from this study, it is reasonable to hypothesize that the MAPK signaling pathway may be involved in the response of chondrosarcoma SW1353 cells to ¹²⁵I seed irradiation.

Limitations

In this study, we selected 10 miRNA and 10 predicted target mRNA genes for verification. However, there may be other miRNAs that should be further studied in the future. In addition, the specific regulatory mechanisms of miRNAs require more attention in future studies. Lastly, additional studies are necessary to further uncover the roles of differentially expressed miRNAs in chondrosarcoma cells.

Conclusions

In summary, our study demonstrated that irradiation from ¹²⁵I seeds effectively inhibits the proliferation of chondrosarcoma cells in vitro, leading to dysregulation of critical miRNAs. The effect of radiation was dose dependent, with higher radiation doses causing more cell growth inhibition. Optimal cell growth inhibition was reached by 7 days postexposure. Next, miR-1224-5p, miR-492, miR-135b-5p, and miR-6839-5p were found to play important roles in the inhibition of proliferation after exposure to radiation. *VEGFA*, *CXCL12*, *MAP4K3*, and *BCL2L14* were identified as potential target genes of the miRNAs. In addition, the MAPK signaling pathway might be involved in how cells respond to irradiation. Our findings presented here provide insight into the effects of ¹²⁵I seed irradiation on chondrosarcoma cells, along with the regulatory roles of miRNAs in SW1353 cells exposed to radiation.

Authors' Note

Fusheng Li and Jia Xu contributed equally to this work.

Acknowledgments

The authors sincerely thank Mr Xiaosong Yang and Mr Yukun Jin for manufacturing the polystyrene pillar and steel cylindrical container for the ¹²⁵I seed irradiator.

Declaration of Conflicting Interests

The author(s) declared no potential conflicts of interest with respect to the research, authorship, and/or publication of this article.

Funding

The author(s) disclosed receipt of the following financial support for the research, authorship, and/or publication of this article: This research was supported by the Liaoning Province Natural Science Foundation of China (no. 20170540518).

References

- Gelderblom H, Hogendoorn PC, Dijkstra SD, et al. The clinical approach towards chondrosarcoma. *Oncologist*. 2008;13(3):320-329. doi:10.1634/theoncologist.2007-0237.
- van Maldegem AM, Gelderblom H, Palmerini E, et al. Outcome of advanced, unresectable conventional central chondrosarcoma. *Cancer*. 2014;120(20):3159-3164. doi:10.1002/cncr.28845.
- Ren C, Zeng J, Song Y, Wang X. Recurrent primary lumbar vertebra chondrosarcoma: marginal resection and iodine-125 seed therapy. *Indian J Orthop*. 2014;48(2):216-219. doi:10.4103/0019-5413.128772.
- Huo X, Wang H, Yang J, et al. Effectiveness and safety of CT-guided (125) I seed brachytherapy for postoperative locoregional recurrence in patients with non-small cell lung cancer. *Brachytherapy*. 2016;15(3):370-380. doi:10.1016/j.brachy.2016.02.001.
- Yuan D, Gao Z, Zhao J, Zhang H, Wang J. ¹²⁵I seed implantation for hepatocellular carcinoma with portal vein tumor thrombus: a systematic review and meta-analysis. *Brachytherapy*. 2019;18(4):521-529. doi:10.1016/j.brachy.2019.01.014.
- Galego P, Silva FC, Pinheiro LC. Analysis of monotherapy prostate brachytherapy in patients with prostate cancer. Initial PSA and Gleason are important for recurrence? *Int Braz J Urol*. 2015;41(2):353-359. doi:10.1590/S1677-5538.
- Li Q, Liang Y, Zhao Y, Gai B. Interpretation of adverse reactions and complications in Chinese expert consensus of iodine-125 brachytherapy for pancreatic cancer. *J Cancer Res Ther*. 2019;15(4):751-754. doi:10.4103/jcrt.JCRT_884_18.
- Nachbichler SB, Kreth FW. Brachytherapy of intracranial gliomas. *Prog Neurol Surg*. 2018;31:72-86. doi:10.1159/000467114.
- Bartel DP. MicroRNAs: genomics, biogenesis, mechanism, and function. *Cell*. 2004;116(2):281-297.
- Cui Q, Yu Z, Pan Y, Purisima EO, Wang E. MicroRNAs preferentially target the genes with high transcriptional regulation complexity. *Biochem Biophys Res Commun*. 2007;352(3):733-738.
- Xi JJ. MicroRNAs in cancer. *Cancer Treat Res*. 2013;158:119-137. doi:10.1007/978-3-642-31659-3_5.
- Yoshitaka T, Kawai A, Miyaki S, et al. Analysis of microRNAs expressions in chondrosarcoma. *J Orthop Res*. 2013;31(12):1992-1998. doi:10.1002/jor.22457.
- Hu C, Cheng X, MingYu Q, Wang XB, Shen SQ. The effects of microRNA-1224-5p on hepatocellular carcinoma tumor endothelial cells. *J Cancer Res Ther*. 2019;15(2):329-335. doi:10.4103/jcrt.JCRT_40_18.

14. Qian J, Li R, Wang YY, et al. MiR-1224-5p acts as a tumor suppressor by targeting CREB1 in malignant gliomas. *Mol Cell Biochem.* 2015;403(1-2):33-41. doi:10.1007/s11010-015-2334-1.
15. Shi LP, Liang M, Li FF, et al. MiR-492 exerts tumor-promoting function in prostate cancer through repressing SOCS2 expression. *Eur Rev Med Pharmacol Sci.* 2019;23(3):992-1001. doi:10.26355/eurrev_201902_16986.
16. Jiang J, Zhang Y, Yu C, Li Z, Pan Y, Sun C. MicroRNA-492 expression promotes the progression of hepatic cancer by targeting PTEN. *Cancer Cell Int.* 2014;14(1):95. doi:10.1186/s12935-014-0095-7.
17. von Frowein J, Hauck SM, Kappler R, et al. MiR-492 regulates metastatic properties of hepatoblastoma via CD44. *Liver Int.* 2018;38(7):1280-1291. doi:10.1111/liv.13687.
18. Liu M, An J, Huang M, et al. MicroRNA-492 overexpression involves in cell proliferation, migration, and radiotherapy response of cervical squamous cell carcinomas. *Mol Carcinog.* 2018;57(1):32-43. doi:10.1002/mc.22717.
19. Gao S, Zhou F, Zhao C, et al. Gastric cardiac adenocarcinoma microRNA profiling in Chinese patients. *Tumour Biol.* 2016;37(7):9411-9422. doi:10.1007/s13277-016-4824-5.
20. Han X, Saiyin H, Zhao J, et al. Overexpression of miR-135b-5p promotes unfavorable clinical characteristics and poor prognosis via the repression of SFRP4 in pancreatic cancer. *Oncotarget.* 2017;8(37):62195-62207. doi:10.18632/oncotarget.19150.
21. Shao L, Chen Z, Soutto M, et al. *Helicobacter pylori*-induced miR-135b-5p promotes cisplatin resistance in gastric cancer. *FASEB J.* 2019;33(1):264-274. doi:10.1096/fj.201701456RR.
22. Zhang Y, Xia F, Zhang F, et al. MiR-135b-5p enhances doxorubicin-sensitivity of breast cancer cells through targeting anterior gradient 2. *J Exp Clin Cancer Res.* 2019;38(1):26. doi:10.1186/s13046-019-1024-3.
23. Sun X, Wei L, Chen Q, Terek RM. MicroRNA regulates vascular endothelial growth factor expression in chondrosarcoma cells. *Clin Orthop Relat Res.* 2015; 473(3):907-913. doi:10.1007/s11999-014-3842-0.
24. de Jong Y, Ingola M, Briaire-de Bruijn IH, et al. Radiotherapy resistance in chondrosarcoma cells; a possible correlation with alterations in cell cycle related genes. *Clin Sarcoma Res.* 2019; 9:9. doi:10.1186/s13569-019-0119-0.
25. Jeong W, Kim H-J. Biomarkers of chondrosarcoma. *J Clin Pathol.* 2018;71(7):579-583. doi:10.1136/jclinpath-2018-205071.
26. Palmi G, Marini F, Brandi ML. What is new in the miRNA world regarding osteosarcoma and chondrosarcoma? *Molecules.* 2017;22(3):E417. doi:10.3390/molecules22030417.
27. Polychronidou G, Karavasilis V, Pollack SM, Huang PH, Lee A, Jones RL. Novel therapeutic approaches in chondrosarcoma. *Future Oncol.* 2017;13(7):637-648. doi:10.2217/fon-2016-0226.
28. Aird EG, Folkard M, Mayes CR, Bownes PJ, Lawson JM, Joiner MC. A purpose-built iodine-125 irradiation plaque for low dose rate energy irradiation of cell lines in vitro. *Br J Radiol.* 2001; 74(877):56-61.
29. Zhang T, Guo J, Gu J, et al. Identifying the key genes and microRNAs in colorectal cancer liver metastasis by bioinformatics analysis and in vitro experiments. *Oncol Rep.* 2019;41(1): 279-291. doi:10.3892/or.2018.6840.
30. Afonso-Grunz F, Müller S. Principles of miRNA-mRNA interactions: beyond sequence complementarity. *Cell Mol Life Sci.* 2015;72(16):3127-3141. doi:10.1007/s00018-015-1922-2.
31. Kim DW, Seo SW, Cho SK, et al. Targeting of cell survival genes using small interfering RNAs (siRNAs) enhances radiosensitivity of grade II chondrosarcoma cells. *J Orthop Res.* 2007;25(6): 820-828.
32. Van Oosterwijk JG, de Jong D, van Ruler M, et al. Three new chondrosarcoma cell lines: one grade III conventional central chondrosarcoma and two dedifferentiated chondrosarcomas of bone. *BMC Cancer.* 2012;12(1):10.
33. Hamdi DH, Barbieri S, Chevalier F, et al. In vitro engineering of human 3D chondrosarcoma: a preclinical model relevant for investigations of radiation quality impact. *BMC Cancer.* 2015; 15(2):579. doi:10.1186/s12885-015-1590-5.
34. Dent P, Yacoub A, Fisher PB, Hagan MP, Grant S. MAPK pathways in radiation responses. *Oncogene.* 2003;22(37):5885-5896.